



A continuum surface model for flows driven by interfacial tension gradients

H. Haj-Hariri,^a Q. Shi,^b A. Borhan^b

^aDepartment of Mechanical and Aero. Engineering, University of Virginia, Charlottesville, VA 22903, USA

^bDepartment of Chemical Engineering, Pennsylvania State University, University Park, PA 16802, USA

Abstract

A new method for the simulation of free-surface flows driven by interfacial tension gradients is discussed. The numerical method is based on a continuum model for interfaces and incorporates oct-tree adaptive refinement of the underlying cartesian grid in order to track the interface without the need for interface reconstruction. This method is then applied to the study of thermocapillary motion of drops the presence of momentum and energy convection.

1 Introduction

Flows driven by interfacial tension gradients have received considerable attention during the past decade due to their significant impact on space-based materials processing applications. Interfacial tension gradients resulting from nonuniform distributions of temperature, surfactant concentration, or charge density on an interface are known to give rise to unbalanced tangential stresses which lead to fluid motion [1]. The resulting motion can play a major role under microgravity conditions where sedimentation and buoyancy-driven convection are largely eliminated. For example, it can provide a mechanism for the movement of drops and bubbles, as was first shown by Young et al. [2]. These authors derived the following expression for the thermally-driven (thermocapillary) migration velocity of a spherical drop of radius a in a constant temperature gradient,



\mathbf{G} , within an unbounded fluid medium:

$$\mathbf{U}_{\text{YGB}} = - \left[\frac{2a(\partial\sigma/\partial T)}{\mu(\kappa + 2)(3\lambda + 2)} \right] \mathbf{G}. \quad (1)$$

In this expression, σ is the interfacial tension, and κ and λ denote the ratios of the thermal conductivity and the viscosity of the drop fluid to those of the surrounding fluid, respectively. Equation (1) is valid so long as the drop remains sufficiently small that convective transport of energy and momentum can be neglected compared to molecular transport of these quantities. Considerable progress has since been made in predicting the thermocapillary migration velocity for systems in which convective effects are significant, as summarized in a recent review article by Subramanian [3]. However, most previous studies of convective effects in this problem have been concerned with the motion of gas bubbles, and have assumed a *fixed spherical shape* for the bubble. Since the terminal velocity of a drop or bubble can be strongly affected by its shape, it is important that drop deformations be taken into account.

The development of efficient and accurate methods for the numerical simulation of such free-surface problems, including finite deformations of the fluid-fluid interfaces, has received considerable attention recently. Some examples include early contributions by Peskin [4], and Hirt and Nichols [5], followed recently by Brackbill et al. [6], Unverdi and Tryggvason [7], Haj-Hariri et al. [8], and Sheth and Pozrikidis [9]. In this paper, we present a general numerical technique for simulating multiphase flows involving nonuniform distributions of interfacial tension at fluid-fluid boundaries, and we apply this method to the study of thermocapillary motion of *deformable* drops in the presence of convective transport of momentum and energy.

2 Governing equations and numerical technique

Consider the thermally-driven motion of a deformable drop in an unbounded incompressible Newtonian fluid. The difficulty in treating this problem lies in the *a priori* unknown location of the drop surface, and the intimate coupling between the evolving temperature distribution and the unknown drop shape, even in the absence of convective effects. This coupling is taken into account by using the idea of continuum modeling of the interface between the drop and the surrounding phase [4, 6]. The continuum surface model is based on the “volume-of-fluid” (VOF) approach of Hirt and Nichols [5], wherein the free surface information is retained by advecting a Lagrangian invariant called the VOF or *color* function. However, it



still requires the costly step of interface reconstruction at every time step in order to overcome the numerical diffusion caused by the relatively coarse underlying uniform cartesian grid. In the present work, an adaptive local grid-refinement scheme is integrated into the continuum surface model to eliminate the need for interface reconstruction. We further incorporate temperature-induced variations of interfacial tension into the model and modify it to allow for the simultaneous solution of the momentum and energy equations.

An important observation based on our numerical results is that the continuum model based on a passively advected color function suffers from the secular loss of integrity of the free surface under conditions where the induced interfacial velocities wash the color function away from the interface. Free-surface problems involving the motion of drops and bubbles are specific examples where such conditions are encountered. This deficiency is addressed by using the level-set idea of Osher and Sethian [10] in a manner similar to that used by Sussman et al. [11], namely by passively advecting a function $s(\mathbf{x})$, denoting the normal distance from the interface ($s = 0$), in the flow field. The small gradients of this function (level set) make the advection process simple. Following Peskin [4], the color function C is then defined as a mollified Heaviside step function based on s , ranging in value from 0 in the 'interior' to 1 in the 'exterior', with a sharp gradient over a thin 'interface region'. The selected thickness of the smeared interface will depend on the desired/available resolution. Based on the level-set function, the surface normal can be generalized as $\mathbf{n} = \nabla s$, so that the stress jump, \mathbf{f} , across the interface, given by

$$\mathbf{f} = \left[\left(-\frac{\partial \sigma}{\partial T} \right) (\mathbf{I} - \mathbf{nn}) \cdot \nabla T + \sigma \mathbf{n} \nabla \cdot \mathbf{n} \right], \quad (2)$$

may be replaced by its volume-distributed counterpart, \mathbf{F} , defined as

$$\mathbf{F} = \mathbf{f} \delta(s) = \mathbf{f} |\nabla C|, \quad (3)$$

where $\delta(s)$ is the Dirac delta function.

Including the smeared body force \mathbf{F} given by eqn [3], the dimensionless momentum and continuity equations in the presence of interfacial tension take the following forms:

$$\frac{\partial \mathbf{u}}{\partial t} + \mathbf{u} \cdot \nabla \mathbf{u} = \frac{1}{\rho Re} [-\nabla p + \mathbf{F} + \nabla \cdot (\mu \nabla \mathbf{u})], \quad \nabla \cdot \mathbf{u} = 0. \quad (4)$$

The solution of the flow problem also requires a knowledge of the temperature distribution which is governed by:

$$\frac{\partial T}{\partial t} + \mathbf{u} \cdot \nabla T = \frac{1}{Ma} \nabla \cdot (\alpha \nabla T). \quad (5)$$



640 Boundary Elements XVII

The physical variables in these equations are nondimensionalized using the following scales:

$$U^* = \frac{-\sigma_T G a}{\mu_{ex}} \quad T^* = G a \quad t^* = \frac{a}{U^*} \quad P^* = \frac{\mu_{ex} U^*}{a} \quad F^* = \frac{\mu_{ex} U^*}{a^2}$$

The resulting dimensionless parameters are the Reynolds, capillary, and Marangoni numbers defined as $Re = -\sigma_T G a^2 / \mu_{ex} \nu_{ex}$, $Ca = -\sigma_T G a / \sigma_o$, and $Ma = -\sigma_T G a^2 / \mu_{ex} \alpha_{ex}$, respectively, where σ_o and σ_T represent the interfacial tension and its variation with temperature at some reference temperature. The dimensionless density, viscosity, and thermal diffusivity distributions in eqns [4] and [5] are defined as,

$$\rho = \frac{\rho_{in}}{\rho_{ex}} C + (1 - C) \quad \mu = \frac{\mu_{in}}{\mu_{ex}} C + (1 - C) \quad \alpha = \frac{\alpha_{in}}{\alpha_{ex}} C + (1 - C).$$

The basic numerical algorithm for the solution of eqns [4] and [5] is the splitting method consisting of the two steps shown below:

$$\frac{\mathbf{u}^* - \mathbf{u}^n}{\delta t} = -\mathbf{u}^n \cdot \nabla \mathbf{u}^n + \frac{1}{\rho^n Re} [\nabla \cdot (\mu \nabla \mathbf{u}^n) + \mathbf{F}_t^n]. \quad [6]$$

$$\frac{\mathbf{u}^{n+1} - \mathbf{u}^*}{\delta t} = \frac{1}{\rho^n Re} [-\nabla p^{n+1} + \mathbf{F}_n^n]. \quad [7]$$

where the body force \mathbf{F} is decomposed into normal and tangential components \mathbf{F}_n and \mathbf{F}_t , respectively, given by

$$\mathbf{F}_n = \frac{1}{Ca} |\nabla C| \mathbf{n} \nabla \cdot \mathbf{n} \quad \mathbf{F}_t = |\nabla C| (\mathbf{I} - \mathbf{nn}) \cdot \nabla T. \quad [8]$$

The incompressibility of the velocity field at time step $n + 1$ leads to the following poisson equation for the pressure,

$$\nabla \cdot \left[\frac{1}{\rho^n} \nabla p^{n+1} \right] = \frac{Re}{\delta t} \nabla \cdot \mathbf{u}^* + \nabla \cdot \left[\frac{1}{\rho^n} \mathbf{F}_n^n \right]. \quad [9]$$

Following each solution iteration, the level-set function is allowed to propagate passively in the computed velocity field, the deformed shape of the drop is determined, and the color function is reconstructed.

The method described above is not at its best if implemented with inadequate resolution. This was shown by Haj-Hariri et al. [12] who used an analytically tractable model problem to examine the effect of the smearing of fluid properties and interfacial force on some global variables of the problem, namely the interfacial velocity (analogous to the migration velocity here). That study indicated a much stronger dependence of the solution on the smearing of the interfacial force as opposed to that of the other fluid properties. Hence, there is a vital need for enhanced resolution in the

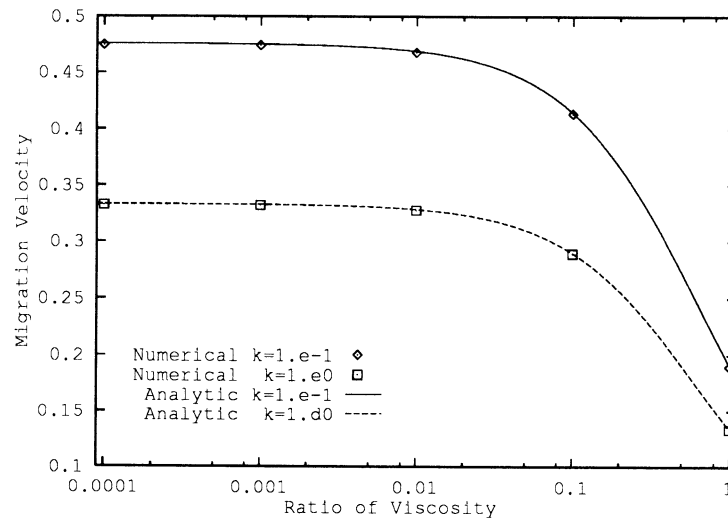
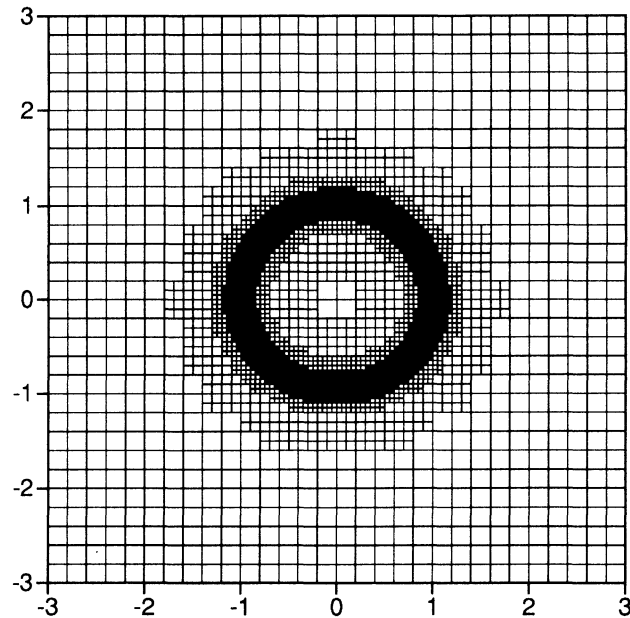


Figure 1: Thermocapillary migration velocity vs. viscosity ratio

implementation of the aforementioned formulation. In order to minimize the computer storage requirements while achieving the desired accuracy, an adaptive local-refinement of the underlying grid was implemented. An important consideration in adaptive schemes is the data structure. In this study, an oct-tree data structure is used wherein 'parent' cells are refined by division into eight 'child' cells. The criterion for refinement of the cartesian grid cells is based on the gradient of the color function C , leading to grid refinement only in the vicinity of the interface. Furthermore, a smooth transition from large cells to small cells is ensured by prohibiting more than a one-level difference between the refinement level of adjacent cells.

3 Numerical results

Several simulations with different values of Re , Ma and Ca are performed to check the effect of these parameters on the deformation of the drop. To avoid the loss of integrity of the interface due to diffusion errors, the level set s is advected instead of the sharply-varying color function. The color function is then redistributed based on the new interface location. For all cases considered, the drop to suspending fluid density, viscosity, and thermal conductivity ratios were fixed at 0.6, 0.7, and 0.1, respectively. The variation of the computed thermocapillary migration velocity with the viscosity ratio, λ , for several values of the thermal conductivity ratio, κ is shown in Fig. 1. These results correspond to simulations performed at

Figure 2: Adapted grid for drop migration ($Re = 1$)

small values of the dynamic governing parameters specified as $Re = 10^{-5}$, $Ma = 10^{-4}$, and $Ca = 7.4 \times 10^{-6}$. The computed migration velocities are in excellent agreement with the analytical results given by equation (1), with errors less than .5%. For these values of the dynamic parameters, the effects of convective transport of momentum and energy are negligible and the drop remains nearly spherical. The computed velocity field also agrees with the analytical results (e.g. Haj-Hariri et al. [13]).

Increasing the Marangoni number alone does not seem to lead to any substantial deformations at $Re = 0$, even for capillary numbers on the order of unity. Hence, we consider instead the effects of the convection of momentum by letting $Re = 1$. The migration velocity for a spherical drop, in the limit of vanishing Re and Ma , is found from Eq. (1) to be 0.232. The perturbation analysis of Haj-Hariri et al. [13] predicts a reduction of the migration velocity, as well as an oblate-spheroidal drop shape. Both of these trends are confirmed by the simulations. Figure 2 contains the final adapted grid for the slightly deformed drop. The calculated migration velocity of the deformed drop is 0.180. Performing the same simulation while constraining the drop shape to remain spherical, the reduction in the migration velocity was found to be 40% less (to a value of 0.203). Therefore, the shape of the drop has a strong influence on its mobility, emphasizing the need for powerful simulation methods that account for finite deformations of the drop shape.

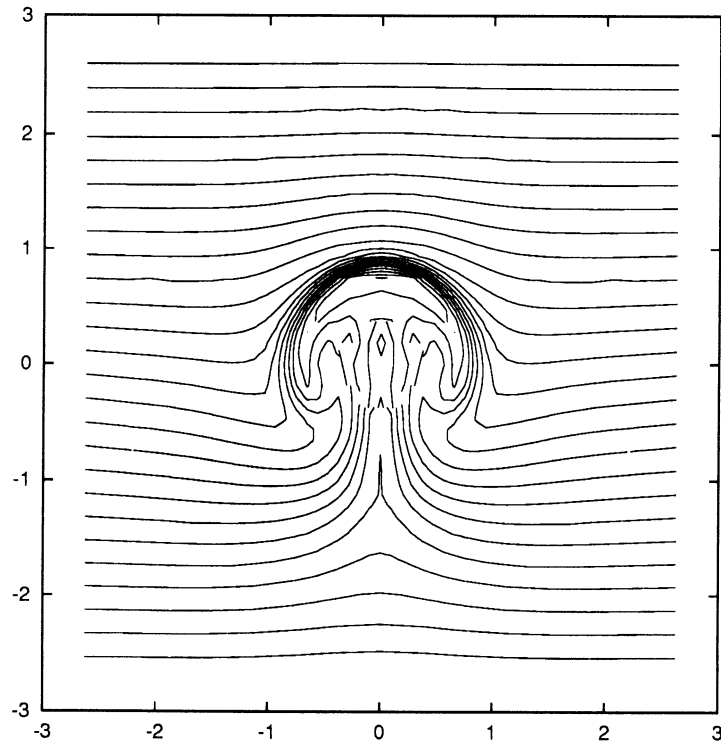


Figure 3: Isotherms for a bubble at $Ma = 100$.

Finally, fully three-dimensional simulations of the thermocapillary motion of a deformable bubble (very small, but nonzero, property ratios) with $Re = 1$ are performed for various values of the Marangoni number. The dependence of the migration velocity on Marangoni number is demonstrated in Table 1, and a representative isotherm contour ($Ma = 100$) in a vertical cut through the domain is given in Fig. 3.

$Ma =$	1	10	100	1000
Present results	0.48	0.36	0.23	0.19
Reference [14]	0.48	0.36	.24	.17

Table 1. Dimensionless migration velocity vs. Ma , for $Re = 1$.

The computed migration velocities for $Re = 1$ seem to be nearly the same as those reported by Balasubramaniam and Lavery [14] for the nondeformable axisymmetric problem.



Acknowledgements

This work was supported by NASA Grant NAG 3-1390 monitored by Dr. Balasubramaniam. The authors acknowledge Dr. Balasubramaniam's assistance.

References

- [1] Levich, V.G. *Physicochemical Hydrodynamics*, Prentice-Hall, Englewood Cliffs, N.J., 1962.
- [2] Young, N.O., Goldstein, J.S. & Block, M.J. The motion of bubbles in a vertical temperature gradient, *J. Fluid Mech.*, 1959, **6**, 350.
- [3] Subramanian, R.S. The motion of bubbles and drops in reduced gravity, *Transport Processes in Drops, Bubbles, and Particles*, ed R. Chhabra & D. Dekee, 1–41, Hemisphere, New York, 1992.
- [4] Peskin, C.S. Numerical analysis of blood flow in the heart, *J. Comp. Phys.*, 1977, **25**, 220–252.
- [5] Hirt, C.W. & Nichols, B.D. Volume of fluid (vof) method for the dynamics of free boundaries, *J. Comp. Phys.*, 1981, **39**, 201–225.
- [6] Brackbill, J.U., Kothe, D.B. & Zemach, C. A continuum method for modeling surface tension, *J. Comp. Phys.*, 1992, **100**, 335–353.
- [7] Unverdi, S.O. & Tryggvason, G. A front-tracking method for viscous, incompressible, multi-fluid flows, *J. Comp. Phys.*, 1992, **100**, 25–37.
- [8] Shi, Q., Haj-Hariri, H. & Borhan, A. Thermocapillary motion of deformable drops, *Bull. Am. Phys. Soc.*, 1993, **38**(12), 2309.
- [9] Sheth, K. & Pozrikidis, C. Effects of inertia on the deformation of liquid drops in simple shear flow, *Computers & Fluids*, 1995, **24**(2), 101–120.
- [10] Osher, S. & Sethian, J.A. Fronts propagating with curvature-dependent speed: Algorithms based on Hamilton-Jacobi formulations, *J. Comput. Phys.*, 1988, **79**, 12.
- [11] Sussman, M., Smereka, P. & Osher, S. A level set approach for computing solutions to incompressible two-phase flow, *J. Comput. Phys.*, 1994, **114**, 146.
- [12] Haj-Hariri, H., Shi, Q. & Borhan, A. Effect of local property smearing on global variables : Implication for numerical simulations of multi-phase flows, *Phys. Fluids*, 1994, **6**(8), 2555.
- [13] Haj-Hariri, H., Nadim, A. & Borhan, A. Effect of inertia on the thermocapillary velocity of a drop, *J. Colloid Interface Sci.*, 1990, **140**, 277.
- [14] Balasubramaniam, R. & Lavery, J.E. Numerical simulation of thermocapillary bubble migration under microgravity for large Reynolds and Marangoni numbers, *Num. Heat Transfer*, 1989, **16**, 175.